Design and Implementation of a Synthetic Biomolecular Concentration Tracker (Supporting Information)

Victoria Hsiao[1*], Emmanuel LC de los Santos[1], Weston R Whitaker[2], John E Dueber[3], and Richard M Murray[1,4]

[1]Division of Biology and Biological Engineering, California Institute of Technology, Pasadena, CA, USA
[2]Department of Microbiology and Immunology, Stanford University, Palo Alto, CA, USA
[3]Department of Bioengineering, University of California, Berkeley, CA, USA
[4]Department of Control and Dynamical Systems, California Institute of Technology, Pasadena, CA, USA
[*]Corresponding Author: V Hsiao, Department of Bioengineering, M/C 138-78, 1200 E California Blvd, Pasadena, CA 91125. Email: vhsiao at caltech.edu.

May 13, 2014

Contents

List of Figures

1 Supplementary Figures

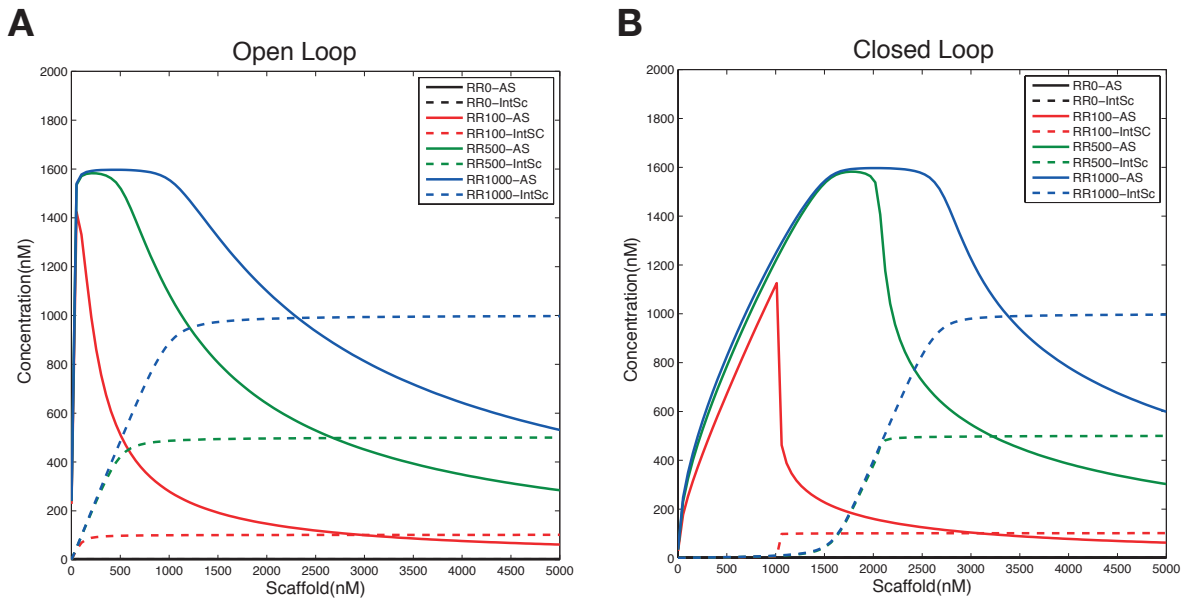

Figure S1: Modeling of single occupancy effect. Dotted lines show intermediate scaffold complexes (labeled as IntSc). IntSc is the sum of Sc:RR, Sc:RR_p,Sc:HK, Sc:HK_p. Solid lines represent antiscaffold concentrations. It is apparent from the model that the drop off in steady stand antiscaffold concentrations corresponds with the increase in intermediate scaffold complexes. This is true for both the open and closed loop circuits. However, the closed loop circuit exhibits this behavior at much higher concentrations of scaffold relative to the open loop.

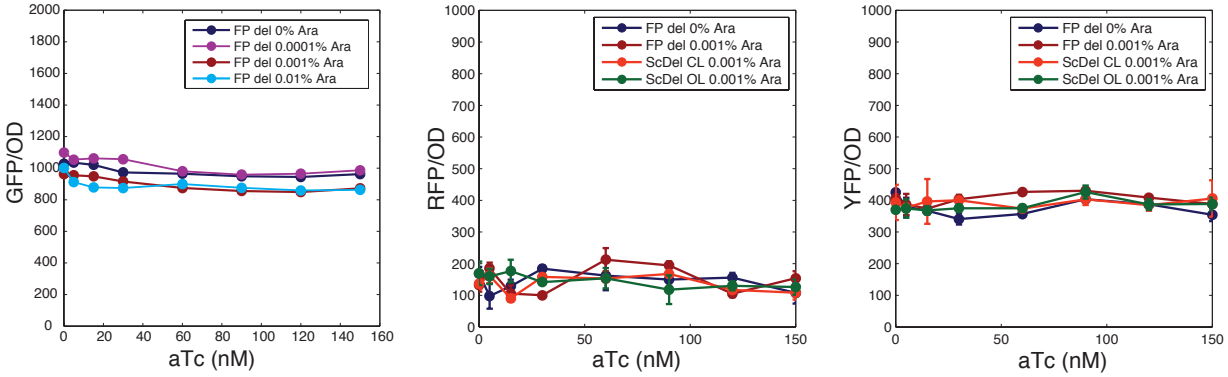

Figure S2: GFP, RFP, and YFP autofluorescence of control *E. coli* strains. *FP del* shows a control strain transformed with the three plasmid system without fluorescence reporters. FP del provides the native autofluorescence of our particular *E. coli* strain, and these values are used for normalization of plate reader data. *Sc Del* is a control strain without the scaffold plasmid, and shows the level cross talk between the HK and RR in the absence of Sc. Auto-fluorescence of the *E. coli* is shown to be independent of arabinose and aTc concentrations.

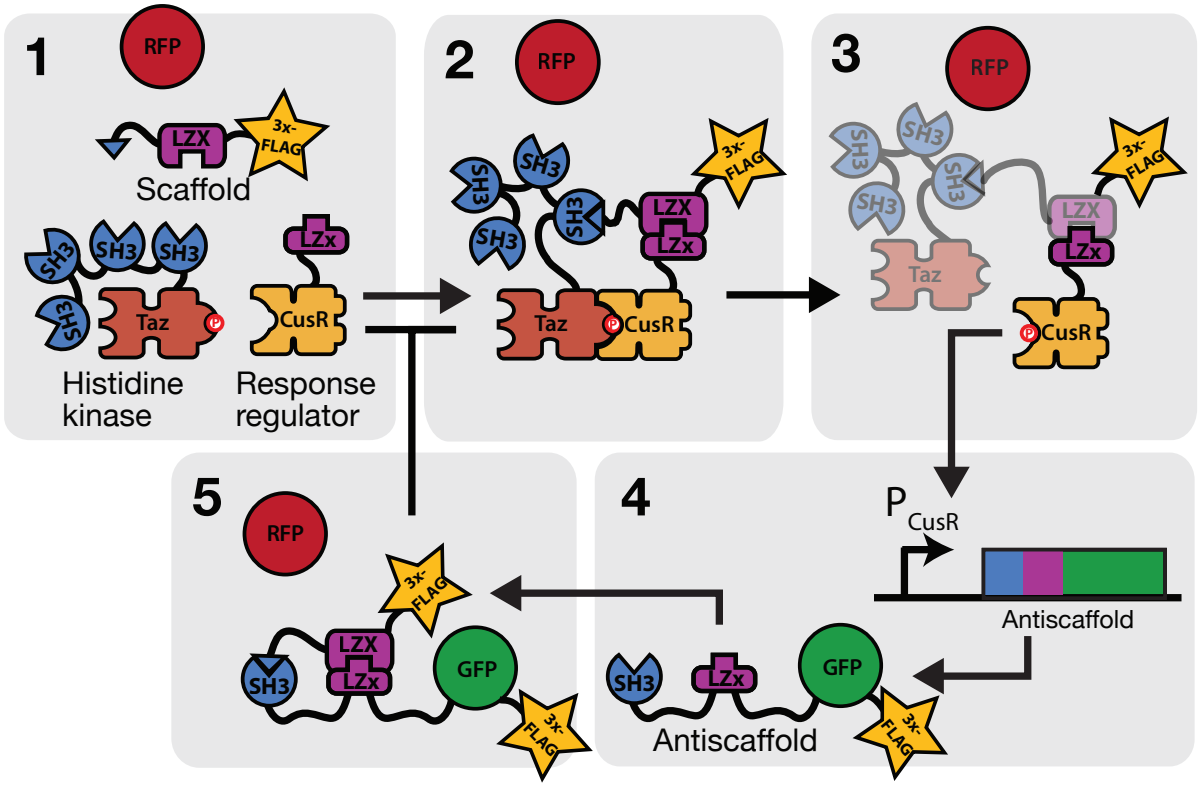

Figure S3: Circuit used for Western blot analysis. The circuit used for western blot analysis has the same architecture as the circuit in Figure 1 of the main text. The main differences are the bicistronic scaffold/mCherry and the use of GFP instead of YFP. mCherry is expressed from its own RBS instead of tethering directly to the scaffold (12 kDa) to provide a substantial size difference from the antiscaffold (44 kDa). The scaffold and antiscaffold are tagged with the 3xFLAG epitope. We expect the addition of the tag not to significantly affect circuit function. None of the molecules have degradation tags and there is no additional phosphatase in the system.

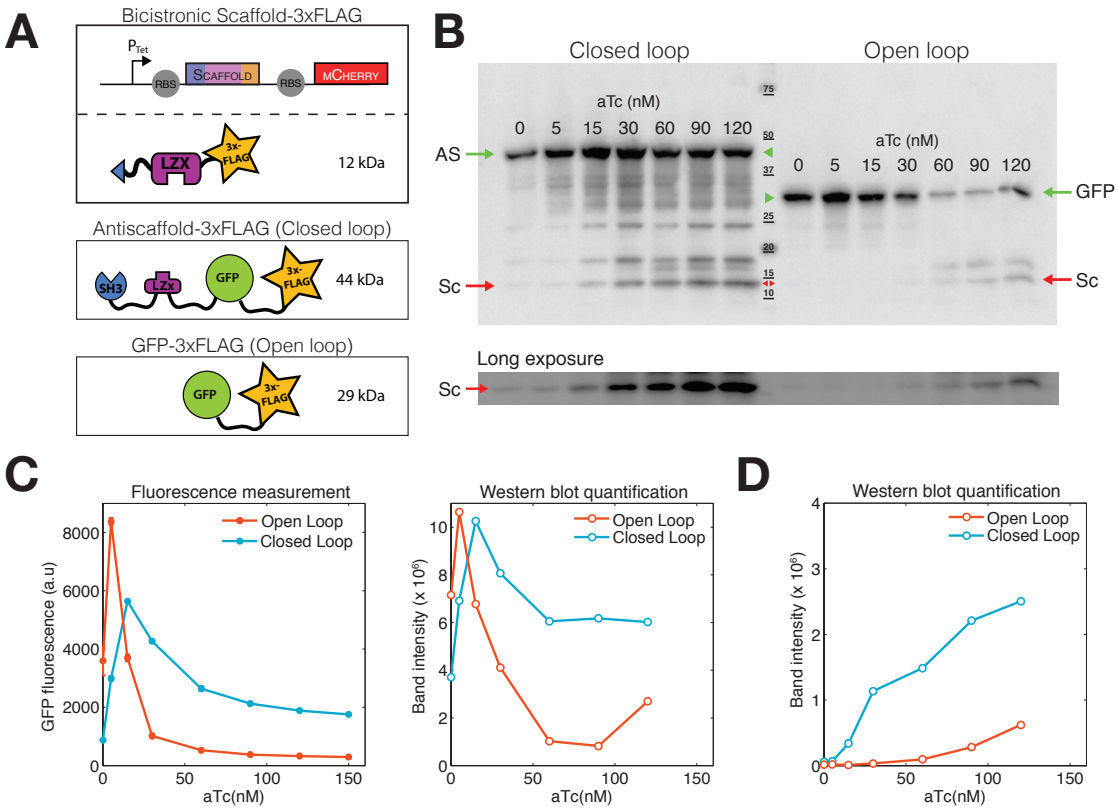

Figure S4: Comparison of fluorescence data to Western blots. A) Both the scaffold and antiscaffold are tagged with the 3xFLAG-tag epitope. The scaffold is expressed on a separate RBS from the mCherry to create a size difference between the scaffold-3xFLAG (12 kDa) and the antiscaffold-GFP-3xFLAG (44 kDa) bands. B) Western blot (15s exposure) of closed loop versus open loop over a range of aTc induction values (0-120 nM). AS denotes antiscaffold band at 44 kDa, Sc denotes scaffold band at 12 kDa, and GFP denotes open loop GFP expression at 29 kDa. Longer exposure (42s) of the blot reveals the scaffold bands more clearly. C) GFP fluorescence versus Western blot quantification of antiscaffold-GFP-3xFLAG. Western blot results for the closed loop versus open loop circuits (Figure 3B) show bands at the expected molecular weights, with significantly darker bands for the antiscaffold (CL) / GFP (OL) than the scaffold (15s exposure). The fluorescence measurements of the experimental cultures were taken immediately prior to lysis for protein blotting. Comparison of GFP/OD and antiscaffold band intensity as a function of aTc induction shows very good agreement in output curves between measured fluorescence and antiscaffold concentrations in both the open and closed loop circuits. D) Western blot quantification of the scaffold-3xFLAG. Measured RFP/OD and band intensity of scaffold cannot be compared since RFP expression is independent of scaffold expression. The discrepancy between open loop and closed loop scaffold expression is due to sequestration of the scaffold in the Sc:AS complex, which we believe protects the scaffold from degradation in the closed loop circuit.

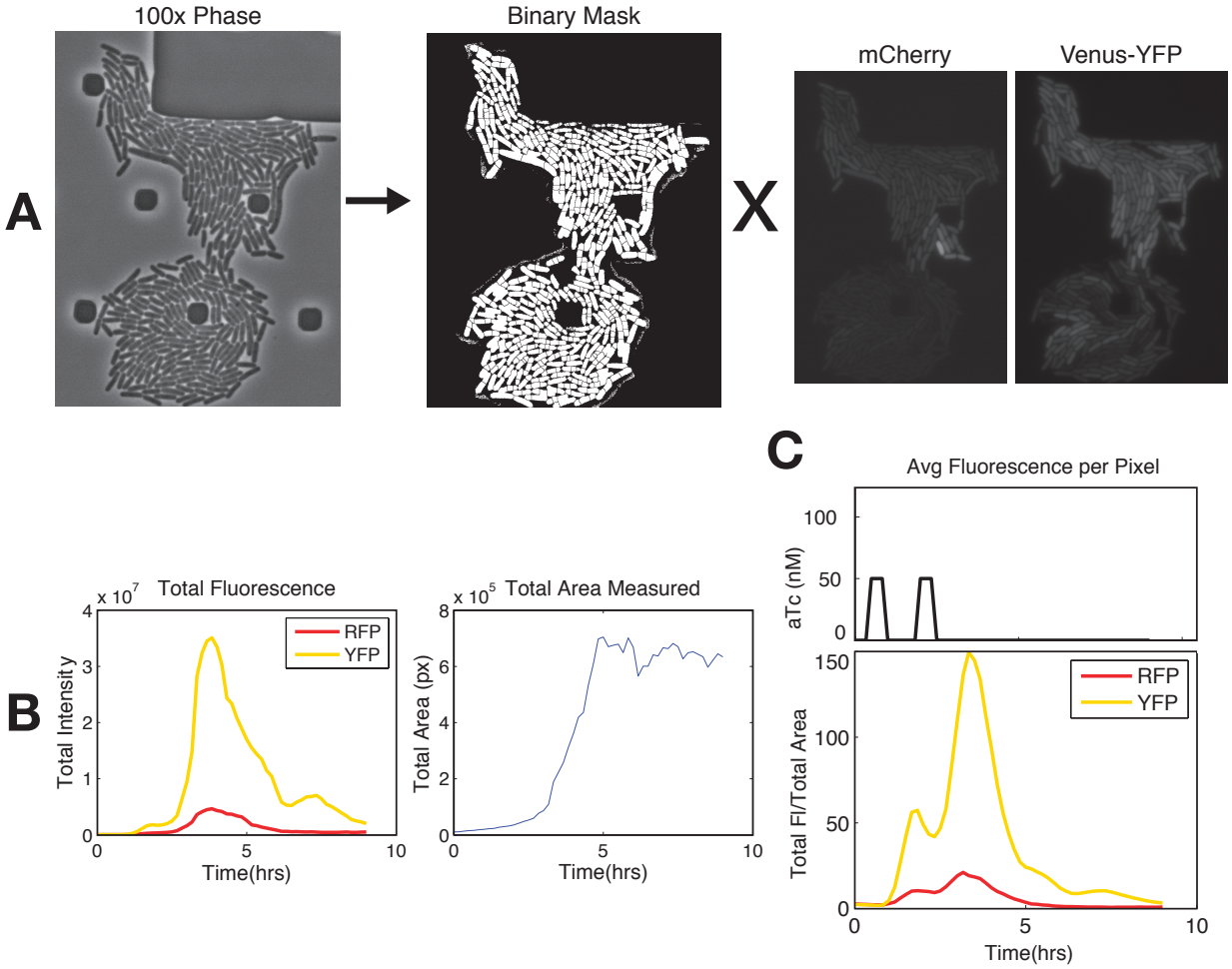

Figure S5: Microscopy analysis overview. A) 100x phase images are converted into binary masks. CellAsic plate features such as the small and large square pillars shown in the figure, are filtered out in ImageJ. The remaining cell segmentation is saved as a binary .PNG file. The binary image is converted into a matrix in MATLAB, and used to extract only cell fluorescence from mCherry and Venus-YFP channels. The fluorescence background average is calculated from the area outside the mask and subtracted from every subsequent frame. B) Total RFP and YFP fluorescence and total cell area are extracted from each frame. C) The total fluorescence is divided by total area to find average fluorescence per pixel. The fluorescence traces shown in Figures 3, 4, and 5 are derived by averaging the average fluorescence per pixel of each frame, with an average of 5-7 frames per experimental condition. Microscopy analysis protocol based on a protocol established by the Phillips group at Caltech (`http://www.rpgroup.caltech.edu/courses/PBL/bootcamp2011/protocols_and_references/Matlab_Tutorial_2010.pdf`).

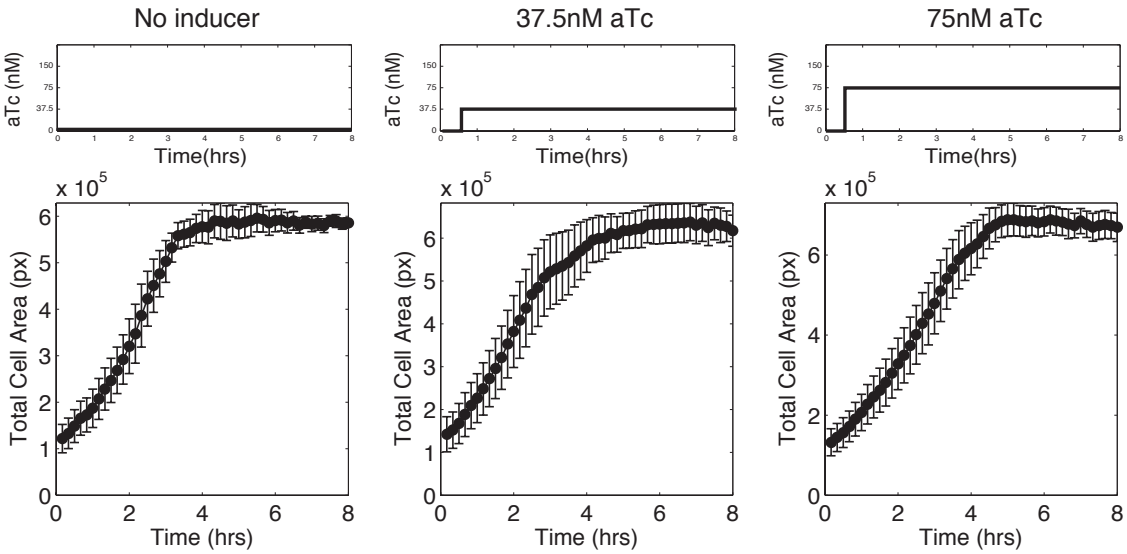

Figure S6: Growth curves for step induction experiment shown in Figure 3 of the main text. Shown is the quantified total cell area extracted from phase contrast microscopy images.

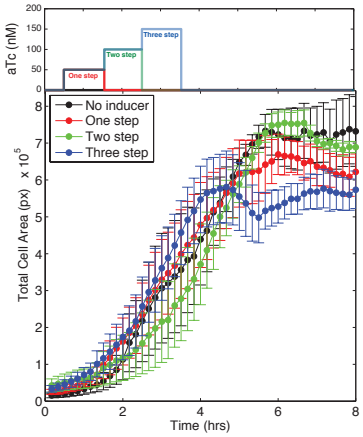

Figure S7: Growth curves for multi-step induction experiment shown in Figure 4 of the main text. Shown is the quantified total cell area extracted from phase contrast microscopy images.

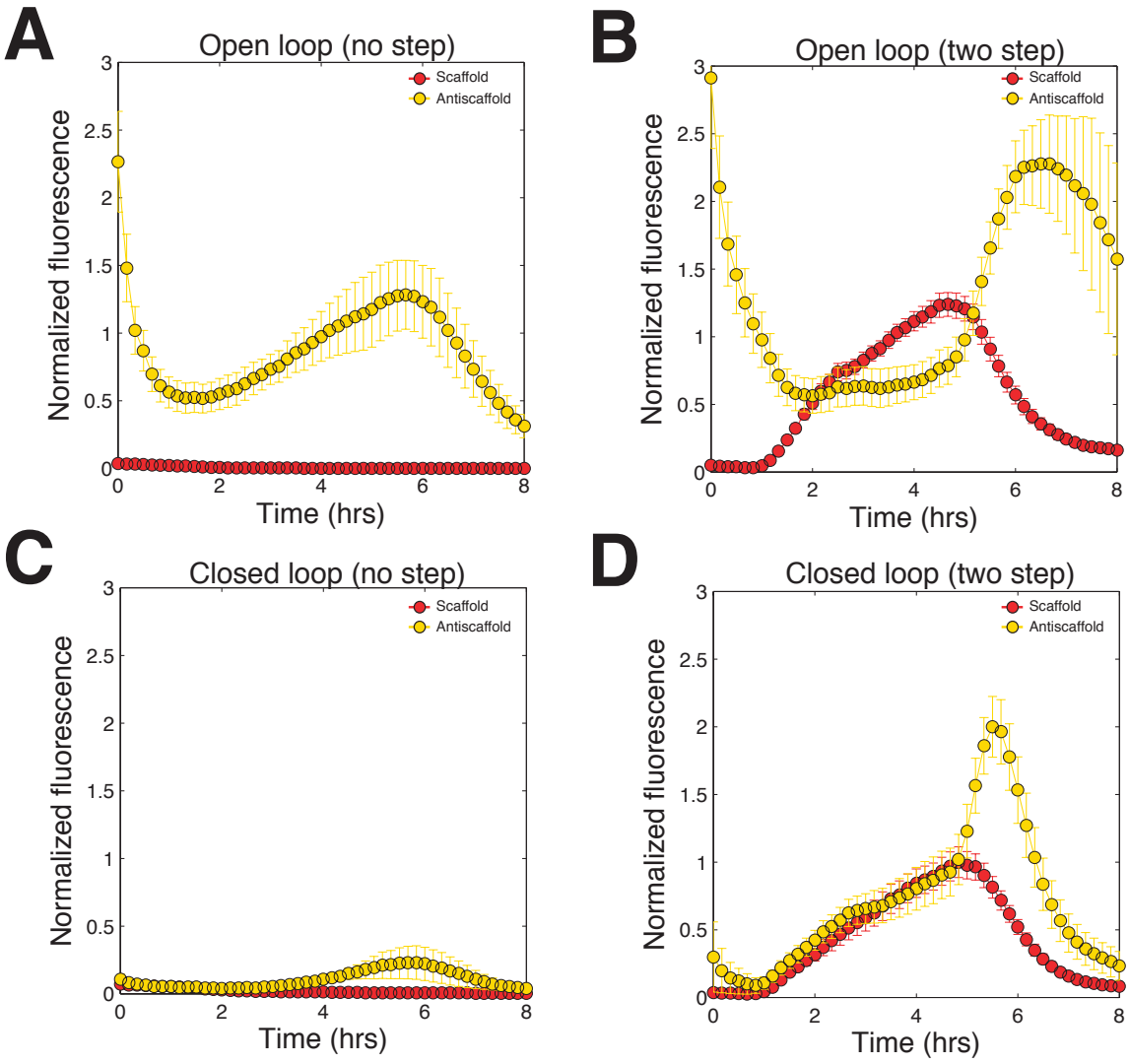

Figure S8: A) Open loop circuit with no aTc induction. Red trace is scaffold-mCherry, yellow traces is antiscaffold-Venus. B) Open loop circuit with 30 minutes of media only, followed by 2 hours of media with 50 nM aTc, followed by 2 hours of 150 nM aTc, then back to media only. C) Closed loop circuit with no aTc induction. D) Closed loop circuit with two step induction described in (B). Fluorescence traces for all four panels are normalized by the closed loop maximum values. RFP is normalized by $\text{clRFP}_{\text{max}}$ and YFP is normalized by $\text{clYFP}_{\text{max}}/2$.

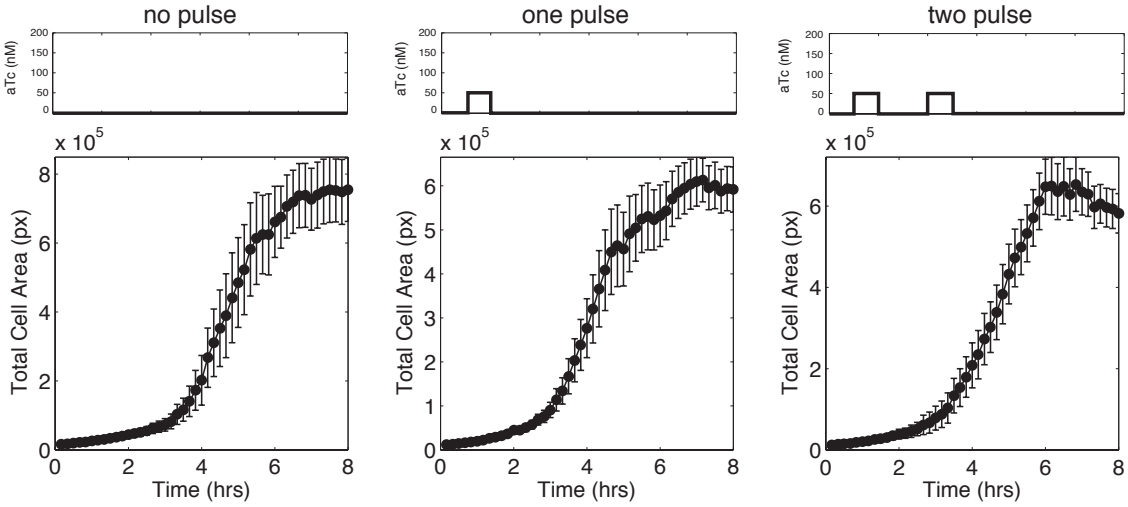

Figure S9: Growth curves for oscillating induction experiment shown in Figure 7 of the main text. Shown is the quantified total cell area extracted from phase contrast microscopy images.

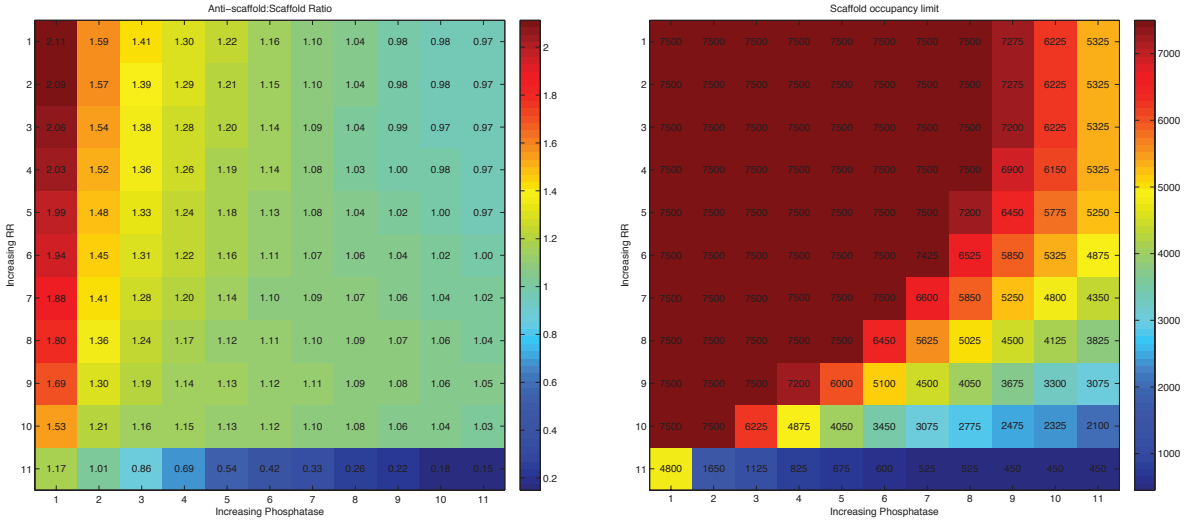

Figure S10: Heat maps from parameter space exploration with values shown. The model was used to find the antiscaffold to scaffold ratio as well as the scaffold occupancy limit over an 11 x 11 matrix of response regulator and phosphatase values. Both RR and Ph values cover the range of 0 to 100 nM in 10 nM increments.

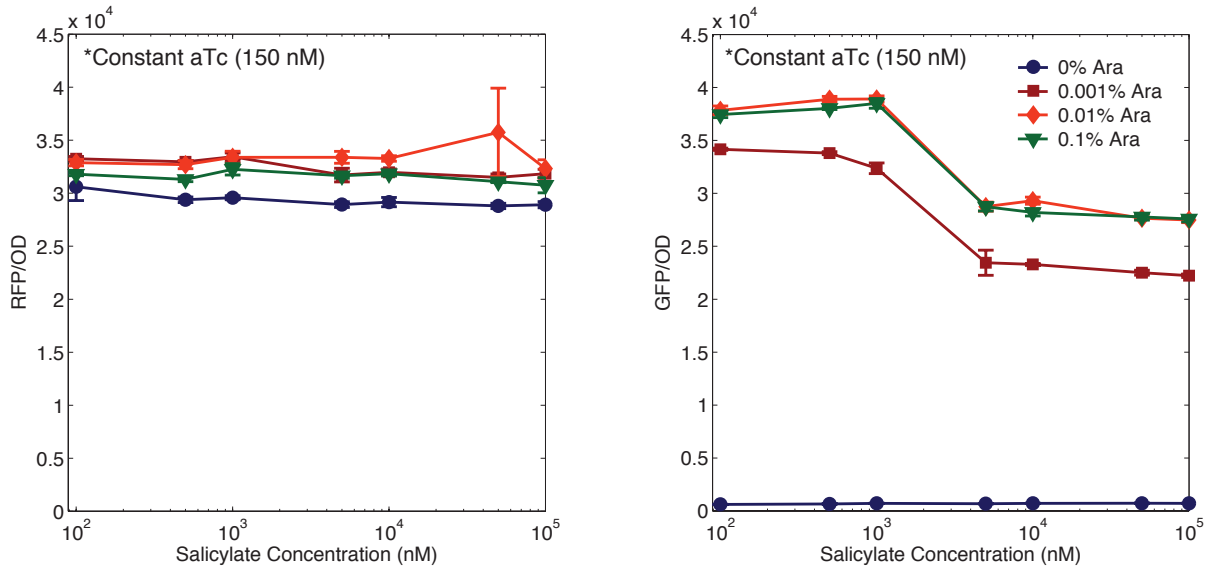

Figure S11: P_{sal} response curve is shown over a range of salicylate levels (0, 1, 10, 100uM). The circuit used was an open loop circuit with P_{sal}-CusS(G448A) and P_{CusR}-GFP. RFP represents scaffold-mCherry, and GFP is the open loop output (no antiscaffold). As salicylate concentration increases, induction of CusS(G448A) phosphatase concentration increases. Increased CusS(G448A) activity decreases concentrations of activated CusR response regulator resulting in lowering levels of GFP.

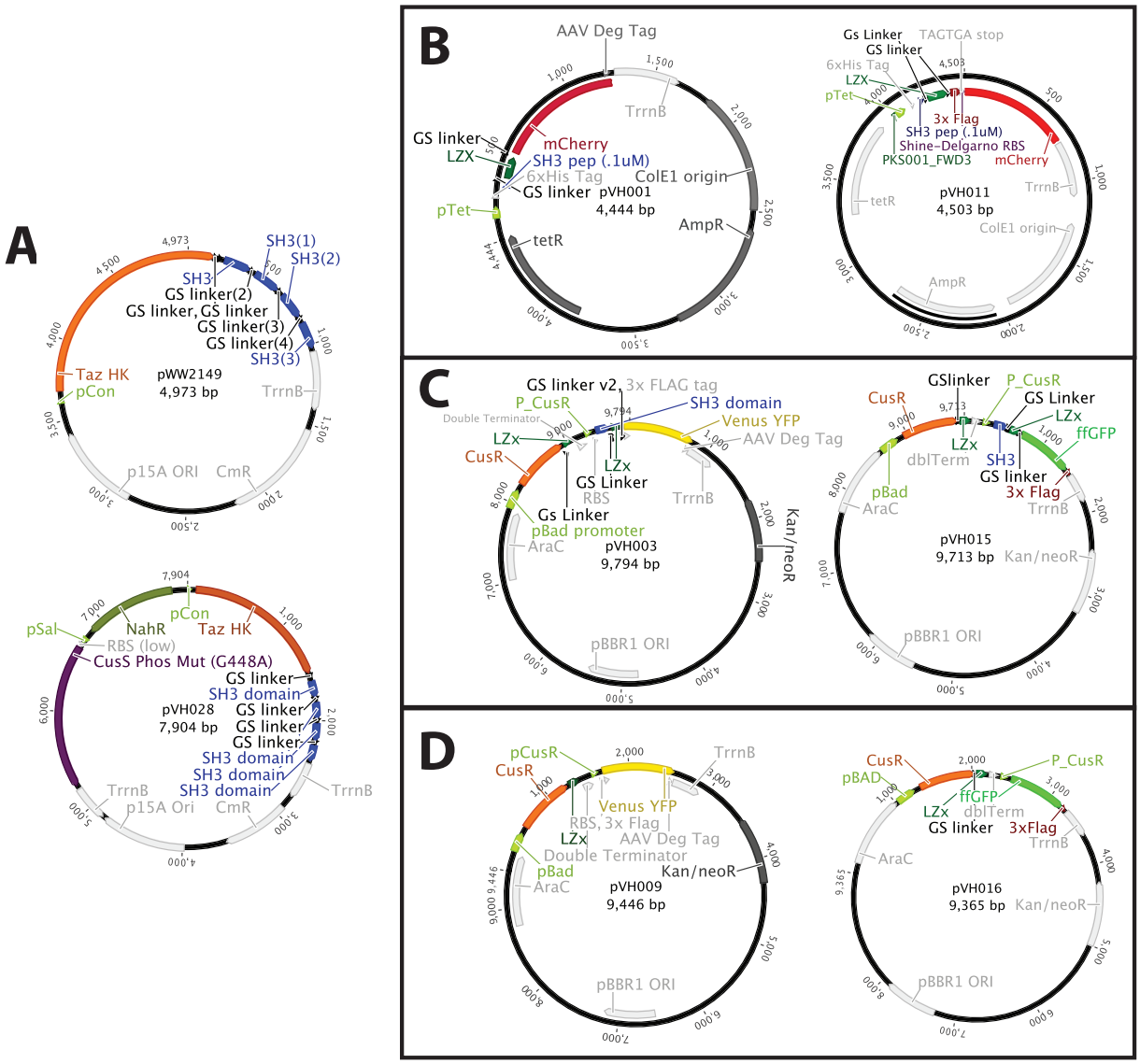

Figure S12: Plasmids used in experimental work. A) Histidine kinase plasmids. pWW2149 has the Taz chimeric histidine kinase with four SH3 binding domains behind a constitutive promoter. pVH028 has the mutated phosphatase, CusS mut G448A, behind an inducible pSal promoter in addition to the Taz HK. Backbone is p15A ori with CmR. B) Scaffold plasmids. pVH001 contains the scaffold-mCherry-AAV fusion behind an inducible pTet promoter. pVH011 contains the bicistronic scaffold/mCherry. Backbone is ColE1 with AmpR. C) Closed loop antiscaffold plasmids. pVH003 contains the response regulator, CusR, behind a pBAD promoter, as well as the antiscaffold-YFP behind the pCusR promoter. pVH015 has a fast-folding GFP reporter(ffGFP) (instead of YFP) with no degradation tag. D) Open loop antiscaffold plasmids. pVH009 is the open loop version of pVH003, in which the sequence for the antiscaffold has been deleted, and only pCusR-YFP remains. pVH016 has ffGFP reporter (instead of YFP) with no degradation tag. Plasmid maps generated with the software Geneious (version 6.1 created by Biomatters).

2 Total list of chemical equations used in model

Mass Action Reactions

Production and Degradation Reactions (other species are degraded with rate γ and not produced)

$$\phi \underset{\gamma}{\overset{HK_{tot}\gamma}{\rightleftharpoons}} HK \tag{1}$$

$$\phi \underset{\gamma}{\overset{RR_{tot}\gamma}{\rightleftharpoons}} RR \tag{2}$$

$$\phi \underset{\gamma}{\overset{Sc_{tot}\gamma}{\rightleftharpoons}} Sc \tag{3}$$

$$\phi \underset{\gamma}{\overset{Ph_{tot}\gamma}{\rightleftharpoons}} Ph \tag{4}$$

Autophosphorylation of histidine kinase

$$HK \underset{k_{rHK_p}}{\overset{k_{fHK_p}}{\rightleftharpoons}} HK_p \tag{5}$$

$$Sc:HK \underset{k_{rHK_p}}{\overset{k_{fHK_p}}{\rightleftharpoons}} Sc:HK_p \tag{6}$$

$$Sc:HK:RR \underset{k_{rHK_p}}{\overset{k_{fHK_p}}{\rightleftharpoons}} Sc:HK_p:RR \tag{7}$$

Non-scaffold mediated background phosphorylation

$$HK_p + RR \underset{k_{rNonCog}}{\overset{k_{fNonCog}}{\rightleftharpoons}} HK + RR_p \tag{8}$$

Scaffold binding to HK-SH3 or RR-LZX

$$Sc + HK \underset{k_{rSc:HK}}{\overset{k_{fSc:HK}}{\rightleftharpoons}} Sc:HK \tag{9}$$

$$Sc + HK_p \underset{k_{rSc:HK}}{\overset{k_{fSc:HK}}{\rightleftharpoons}} Sc:HK_p \tag{10}$$

$$Sc + RR \underset{k_{rSc:RR}}{\overset{k_{fSc:RR}}{\rightleftharpoons}} Sc:RR \tag{11}$$

$$Sc + RR_p \underset{k_{rSc:HK}}{\overset{k_{fSc:HK}}{\rightleftharpoons}} Sc:RR_p \tag{12}$$

Trimer formation

$$Sc:HK + RR \underset{k_{rSc:RR}}{\overset{k_{fSc:RR}}{\rightleftharpoons}} Sc:HK:RR \tag{13}$$

$$Sc:HK_p + RR \underset{k_{rSc:RR}}{\overset{k_{fSc:RR}}{\rightleftharpoons}} Sc:HK_p:RR \tag{14}$$

$$Sc:HK + RR_p \underset{k_{rSc:RR}}{\overset{k_{fSc:RR}}{\rightleftharpoons}} Sc:HK:RR_p \tag{15}$$

$$Sc:HK_p + RR + p \underset{k_{rSc:RR}}{\overset{k_{fSc:RR}}{\rightleftharpoons}} Sc:HK_p:RR_p \tag{16}$$

$$Sc:RR + HK \underset{k_{rSc:HK}}{\overset{k_{fSc:HK}}{\rightleftharpoons}} Sc:HK:RR \tag{17}$$

$$Sc:RR + HK_p \underset{k_{rSc:HK}}{\overset{k_{fSc:HK}}{\rightleftharpoons}} Sc:HK_p:RR \tag{18}$$

$$Sc:RR_p + HK \underset{k_{rSc:HK}}{\overset{k_{fSc:HK}}{\rightleftharpoons}} Sc:HK:RR_p \tag{19}$$

$$Sc:RR_p + HK_p \underset{k_{rSc:HK}}{\overset{k_{fSc:HK}}{\rightleftharpoons}} Sc:HK_p:RR_p \tag{20}$$

Phosphorylation of Response Regulator

$$ScHK_pRR \underset{k_{rCogP}}{\overset{k_{fCogP}}{\rightleftharpoons}} Sc:HK:RR_p \tag{21}$$

Dephosphorylation of Response Regulator

$$Ph + RR_p \underset{k_{r_{Ph:RR}}}{\overset{k_{f_{Ph:RR}}}{\rightleftharpoons}} Ph:RR_p \xrightarrow{k_{f_{dephos}}} Ph + RR \tag{22}$$

$$Ph + Sc:RR_p \underset{k_{r_{Ph:RR}}}{\overset{k_{f_{Ph:RR}}}{\rightleftharpoons}} Ph:Sc:RR_p \xrightarrow{k_{f_{dephos}}} Ph + ScRR \tag{23}$$

$$Ph + Sc:HK:RR_p \underset{k_{r_{Ph:RR}}}{\overset{k_{f_{Ph:RR}}}{\rightleftharpoons}} Ph:Sc:HK:RR_p \xrightarrow{k_{f_{dephos}}} Ph + ScHKRR \tag{24}$$

$$Ph + Sc:HK_p:RR_p \underset{k_{r_{Ph:RR}}}{\overset{k_{f_{Ph:RR}}}{\rightleftharpoons}} Ph:Sc:HK_p:RR_p \xrightarrow{k_{f_{dephos}}} Ph + Sc:HK_p:RR \tag{25}$$

$$Ph + Sc:RR_p:AS \underset{k_{r_{Ph:RR}}}{\overset{k_{f_{Ph:RR}}}{\rightleftharpoons}} Ph:Sc:RR_p:AS \xrightarrow{k_{f_{dephos}}} Ph + Sc:RR:AS \tag{26}$$

$$\tag{27}$$

Sequestration of Scaffold by Antiscaffold

$$Sc + AS \xrightarrow{k_{f_{ScAS}}} ScAS \tag{28}$$

$$Sc : HK + AS \underset{k_{rAS_{LZX}}}{\overset{k_{fAS_{LZX}}}{\rightleftharpoons}} ScHKAS \xrightarrow{k_{rAS_{SH3}}} Sc : AS + HK \tag{29}$$

$$Sc : HK_p + AS \underset{k_{rAS_{LZX}}}{\overset{k_{fAS_{LZX}}}{\rightleftharpoons}} ScHK_pAS \xrightarrow{k_{rAS_{SH3}}} Sc : AS + HK_p \tag{30}$$

$$Sc : RR + AS \underset{k_{rAS_{SH3}}}{\overset{k_{fAS_{SH3}}}{\rightleftharpoons}} ScRRAS \xrightarrow{k_{rAS_{LZX}}} Sc : AS + RR \tag{31}$$

$$Sc : RR_p + AS \underset{k_{rAS_{SH3}}}{\overset{k_{fAS_{SH3}}}{\rightleftharpoons}} ScRR_pAS \xrightarrow{k_{rAS_{LZX}}} Sc : AS + RR_p \tag{32}$$

Additional Reactions with Phosphatase-bound Complexes

$$Sc + Ph : RR_p \underset{k_{rSc:HK}}{\overset{k_{fSc:HK}}{\rightleftharpoons}} Ph : Sc : RR_p \tag{33}$$

$$Sc : HK + Ph : RR_p \underset{k_{rSc:RR}}{\overset{k_{fSc:RR}}{\rightleftharpoons}} Ph : Sc : HK : RR_p \tag{34}$$

$$Sc : HK_p + Ph : RR_p \underset{k_{rSc:RR}}{\overset{k_{fSc:RR}}{\rightleftharpoons}} Ph : Sc : HK_p : RR_p \tag{35}$$

$$Ph : Sc : RR_p + HK \underset{k_{rSc:HK}}{\overset{k_{fSc:HK}}{\rightleftharpoons}} Ph : Sc : HK : RR_p \tag{36}$$

$$Ph : Sc : RR_p + HK_p \underset{k_{rSc:HK}}{\overset{k_{fSc:HK}}{\rightleftharpoons}} Ph : Sc : HK_p : RR_p \tag{37}$$

$$Ph : Sc : RR_p + AS \underset{k_{rAS_{SH3}}}{\overset{k_{fAS_{SH3}}}{\rightleftharpoons}} Ph : Sc : RR_p : AS \xrightarrow{k_{rAS_{LZX}}} Sc : AS + Ph : RR_p \tag{38}$$

Non-Mass Action - Activation of Antiscaffold Expression

$$\phi \underset{\gamma}{\overset{k_f}{\rightleftharpoons}} As \tag{39}$$

$$k_{fAS} = \beta_{AS}\left[\beta_0 + \left(\frac{\mathrm{RR}^2_{\mathrm{active}}}{\mathrm{K}^2_{\mathrm{D}} + \mathrm{RR}^2_{\mathrm{active}}}\right)\right] \tag{40}$$

where $\mathrm{RR}_{\mathrm{active}} = \mathrm{RR}_{\mathrm{p}} + \mathrm{Sc} : \mathrm{RR}_{\mathrm{p}} + \mathrm{Sc} : \mathrm{HK} : \mathrm{RR}_{\mathrm{p}} + \mathrm{Sc} : \mathrm{HK}_{\mathrm{p}} : \mathrm{RR}_{\mathrm{p}} + \mathrm{Sc} : \mathrm{RR}_{\mathrm{p}} : \mathrm{AS}$.

3 List of plasmids and cell strains used

Plasmids		
Name	Resistance	Description
pWW2149	Chloramphenicol	Contains pCon-Taz (histidine kinase). p15A origin of replication, low copy.
pVH028	Chloramphenicol	Contains pCon-Taz (histidine kinase) and pSal-CusSmut (phosphatase). Also has NahR for the pSal promoter. p15A origin of replication, low copy.
pVH001	Carbenicillin/Amp	Contains pTet-Scaffold-mCherry-AAV and TetR genes. ColE1 origin of replication, high copy.
pVH011	Carbenicillin/Amp	Contains bicistronic pTet-Scaffold(3xFLAG)-ShineDelgarno-mCherry and TetR genes. ColE1 origin of replication, high copy.
pVH003	Kanamycin	Contains pBAD-CusR (response regulator) and pCusR-antiscaffold-YFP-AAV. pBBR1 origin of replication, medium copy.
pVH015	Kanamycin	Contains pBAD-CusR (response regulator) and pCusR-antiscaffold-GFP(3xFLAG). pBBR1 origin of replication, medium copy.
pVH009	Kanamycin	Contains pBAD-CusR (response regulator) and pCusR-YFP-AAV. pBBR1 origin of replication, medium copy.
pVH016	Kanamycin	Contains pBAD-CusR (response regulator) and pCusR-GFP(3xFLAG). pBBR1 origin of replication, medium copy.
pVH002	Carbenicillin/Amp	Contains pTet-Scaffold with no fluorescent protein. Used as a control for autofluorescence.
pVH004	Kanamycin	Contains pBAD-CusR and pCusR-antiscaffold with no fluorescent protein. Used as a control for autofluorescence.

Strains (All in WW62 *E.coli*)		
Name	Plasmids Contained	Description
eVH15	pWW2149/pVH011/pVH015	Closed loop Western blot circuit. Cm/Carb/Kan resistance.
eVH16	pWW2149/pVH011/pVH016	Open loop Western blot circuit. Cm/Carb/Kan resistance.
eVH38	pVH028/pVH001/pVH003	Closed loop tracker circuit. Cm/Carb/Kan resistance.
eVH39	pVH028/pVH001/pVH009	Open loop tracker circuit. Cm/Carb/Kan resistance.
eVH05	pww2149/pVH002/pVH004	Autofluorescence control strain. Cm/Carb/Kan
eVH42	pVH028/pVH003	Scaffold-less closed loop control. Cm/Kan
eVH43	pVH028/pVH009	Scaffold-less open loop control. Cm/Kan